

Nanoscale Impurity Structures on the Surface of $d_{x^2-y^2}$ -wave Superconductors

Nikolaos A. Stavropoulos and Dirk K. Morr

Department of Physics, University of Illinois at Chicago, Chicago, IL 60607

(Dated: November 21, 2018)

We study the effects of nanoscale impurity structures on the local electronic structure of $d_{x^2-y^2}$ -wave superconductors. We show that the interplay between the momentum dependence of the superconducting gap, the geometry of the nanostructure and its orientation gives rise to a series of interesting quantum effects. Among these are the emergence of a zero bias conductance peak in the superconductor's density of states and the suppression of impurity states for certain nanostructures. The latter effect can be used to screen impurity resonances in the superconducting state.

PACS numbers: 73.22.-f, 74.72.-h, 72.10.Fk, 74.25.Jb

The study of impurities in the cuprate superconductors has attracted significant interest over the last few years due to the impurities' dramatic effects on the superconductor's local electronic structure. In particular, fermionic resonance states induced by single, isolated impurities have been well characterized experimentally [1, 2] and investigated theoretically [3, 4] (for a recent review, see Ref. [5]). It was recently argued that quantum interference effects involving two impurities yield new insight into the nature of the electronic correlations in the cuprate superconductors [6]. At the same time, studies of nanoscale impurity structures (so-called quantum corrals) in metals [7, 8, 9] have led to the discovery of exciting quantum effects, such as quantum imaging [7] and similar effects are also predicted to occur in s -wave superconductors [10]. The question thus naturally arises whether nanostructures in $d_{x^2-y^2}$ -wave superconductors give rise to novel quantum effects and provide new information on the cuprates' complex electronic structure.

In this Letter, we address this question and study the effects of nanoscale impurity structures on the local electronic structure of a $d_{x^2-y^2}$ -wave superconductor. We take the nanostructures to be located on the superconductor's surface and to interact with the superconductor's electronic degrees of freedom via a non-magnetic scattering potential. We show that nanostructures induce fermionic resonance states inside the superconducting gap, whose spatial form is determined by the interplay between the momentum dependence of the superconducting gap, the geometry of the nanostructure, and its orientation with respect to the underlying lattice. This interplay leads to a number of interesting quantum effects. First, a zero-bias conductance peak (ZBCP) emerges in the superconductor's density of states (DOS) whose dependence on the nanostructure's orientation provides a new tool for identifying the symmetries of unconventional superconductors. Second, for certain nanostructures, destructive quantum interference leads to a complete suppression of impurity resonances; an effect that can be used to spatially screen impurity resonances in the superconducting state. Third, we demonstrate by using more complex nanostructures, that it is

possible to "custom-design" the spatial form of impurity resonances. This effect potentially provides a new probe for electronic correlations of complex systems in general.

In order to study how a nanostructure affects the superconductor's local electronic structure, we compute the superconductor's real space Greens function within a generalized \hat{T} -matrix scattering theory [11, 12]. Introducing the spinor $\Psi_{\mathbf{r}}^{\dagger} = (c_{\mathbf{r},\uparrow}^{\dagger}, c_{\mathbf{r},\downarrow}^{\dagger})$ the electronic Greens function, $\hat{G}(\mathbf{r}, \mathbf{r}', \tau - \tau') = -\langle \mathcal{T} \Psi_{\mathbf{r}}(\tau) \Psi_{\mathbf{r}'}^{\dagger}(\tau') \rangle$, in Matsubara frequency space is given by

$$\hat{G}(\mathbf{r}, \mathbf{r}', \omega_n) = \hat{G}_0(\mathbf{r}, \mathbf{r}', \omega_n) + \sum_{i,j=1}^N \hat{G}_0(\mathbf{r}, \mathbf{r}_i, \omega_n) \hat{T}(\mathbf{r}_i, \mathbf{r}_j, \omega_n) \hat{G}_0(\mathbf{r}_j, \mathbf{r}', \omega_n), \quad (1)$$

where the sum runs over the locations \mathbf{r}_i ($i = 1, \dots, N$) of the N impurities forming the nanostructure. The \hat{T} -matrix is obtained from the Bethe-Salpeter equation

$$\hat{T}(\mathbf{r}_i, \mathbf{r}_j, \omega_n) = \hat{V}_i \delta_{i,j} + \hat{V}_i \sum_{l=1}^N \hat{G}_0(\mathbf{r}_i, \mathbf{r}_l, \omega_n) \hat{T}(\mathbf{r}_l, \mathbf{r}_j, \omega_n), \quad (2)$$

where $\hat{V}_i = U_i \sigma_3$, U_i is the non-magnetic scattering potential of the impurity at site \mathbf{r}_i , and σ_j are the Pauli matrices. We consider identical impurities and take for definiteness $U_i = 1\text{eV}$, however, the results discussed below remain qualitatively unchanged over a wide range of scattering strength. The electronic Greens function of the unperturbed (clean) superconductor in momentum space is given by

$$\hat{G}_0^{-1}(\mathbf{k}, i\omega_n) = i\omega_n \sigma_0 - \varepsilon_{\mathbf{k}} \sigma_3 + \Delta_{\mathbf{k}} \sigma_1, \quad (3)$$

where $\Delta_{\mathbf{k}} = \Delta_0 (\cos k_x - \cos k_y) / 2$ is the superconducting $d_{x^2-y^2}$ -wave gap with $\Delta_0 = 25$ meV, and

$$\varepsilon_{\mathbf{k}} = -2t (\cos k_x + \cos k_y) - 4t' \cos k_x \cos k_y - \mu \quad (4)$$

is the host system's normal state tight binding dispersion with $t = 300$ meV, $t'/t = -0.4$, and $\mu/t = -1.18$, representative of the cuprate superconductors [13]. The local

DOS, $N(\mathbf{r}, \omega)$, is obtained numerically from Eqs.(1)-(4) with $N(\mathbf{r}, \omega) = -2\text{Im}\hat{G}_{11}(\mathbf{r}, \omega + i\delta)/\pi$ and $\delta = 0.2$ meV.

In order to better understand the dependence of impurity states on the geometry and orientation of a nanostructure, it is necessary to first study how the spatial form of impurity resonances evolves as the size and complexity of a nanostructures increases. As a reference point, we plot in Fig. 1(a) the spatial DOS pattern of the resonance state at $\omega = 0$ meV that is induced by a single impurity located at $\mathbf{r}_1 = (0, 0)$ [light (dark) color indicates a large (small) DOS]. When a second impurity

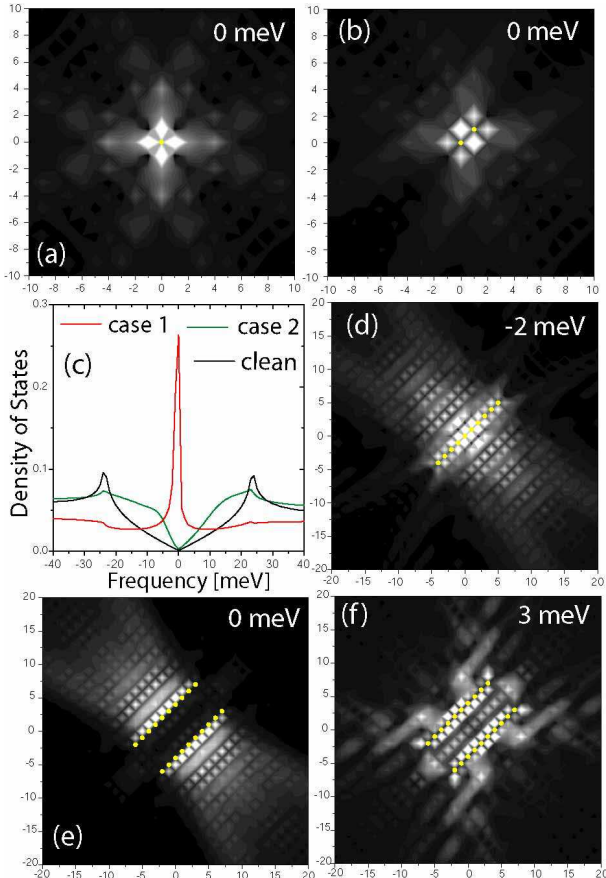


FIG. 1: Intensity plot of the DOS for (a) a single impurity located at $\mathbf{r}_1 = (0, 0)$, (b) two impurities located at \mathbf{r}_1 and $\mathbf{r}_2 = (1, 1)$, (d) $N = 10$ impurities aligned along the (110) -direction, (e),(f) two lines with $N = 10$ impurities each separated by $d = 4\sqrt{2}$ (the lattice constant is set to $a_0 = 1$). (c) DOS as a function of frequency at $(0, 1)$ (see text). Non-magnetic impurities are represented by filled yellow circles.

is added, the mere existence of an impurity state depends on the orientation of this impurity dimer relative to the underlying lattice. If the two impurities are aligned along the (110) -direction (case I), with the second impurity at $\mathbf{r}_2 = (1, 1)$, a resonance state exists at $\omega = 0$ with the spatial DOS structure shown in Fig. 1(b). In contrast, if the second impurity is placed at $\mathbf{r}'_2 = (0, 1)$ (case II) and the dimer is aligned along the (100) -direction, the DOS ex-

hibits only Friedel-like oscillations, but no impurity resonance. This striking difference is particularly apparent when one plots the DOS at $(0, 1)$, as shown in Fig. 1(c). This dependence of the resonance on the dimer's orientation is similar to that of the zero bias conductance peak (ZBCP) observed near one-dimensional surface edges in the cuprate superconductors [14]. Only if the electrons that are specularly scattered along the impurity dimer experience a sign change in the superconducting gap, a ZBCP-like impurity resonance emerges, such as the one shown in Fig. 1(b) for case I. This orientational dependence is an important feature of nanostructures, as further discussed below.

A characteristic signature of the ZBCP-like state is that it extends spatially perpendicular to the impurity line, as shown in Fig. 1(d). Note, however, that the ZBCP-like state is shifted away from zero energy, and located at $\omega = \pm 2$ meV. This shift arises from the hybridization of the ZBCP-like states on both sides of the impurity line, and the resulting formation of bonding and antibonding resonances. This hybridization is mediated by the next-nearest neighbor hopping term (the t' -term), which permits the exchange of electrons between the two sides of the impurity line without a scattering process. When the hybridization of the ZBCP-like states is suppressed, as for example, in the nanostructure consisting of two parallel lines shown in Fig. 1(e), the ZBCP-like state is again located at zero-energy. Here, the ZBCP-like states are spatially separated and the absence of an impurity state between the two lines prevents the coupling of the states and thus their hybridization. A similar effect is also observed for other nanostructures (see below). In addition to a ZBCP-like state, the nanostructure also induces impurity states with different spatial patterns, such as the “frog-like” resonance shown in Fig. 1(f). Quite interestingly, the global spatial pattern of this resonance extends along the (100) -direction, but consists of lines with increased DOS along the (110) -direction. Finally, note that the intensity of the ZBCP-like states decreases algebraically $\sim 1/r^\alpha$ along the (110) -direction with distance from the nanostructure. For the single impurity resonance in Fig. 1(a), one has $\alpha = 2$ [3], while for nanostructures and distances smaller than their lateral size, we find in general $\alpha < 2$. For example, $\alpha \approx 1.18$ for the nanostructure shown in Fig. 1(e). This decrease of α with increasing length of the impurity line is expected since for a truly one-dimensional ZBCP-like state at zero energy, one has $\alpha = 0$.

To further explore the interplay between geometry and orientation, we next consider nanostructures in the form of a square, such as the one shown in Fig. 2 whose sides are parallel to the (110) -direction. This nanostructure induces a ZBCP-like resonance at $\omega = 0$ meV [Fig. 2(a)], which extends in all four equivalent (110) -directions. The ZBCP-like resonances associated with each side are spatially separated and thus do not hybridize. Impurity

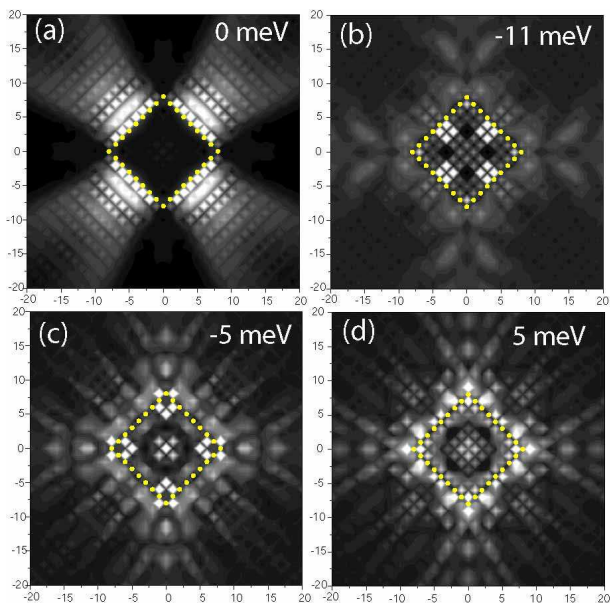


FIG. 2: Intensity plot of the DOS for a square with $N = 32$ impurities and sides of length $a = 8\sqrt{2}$ which are parallel to the (110) and symmetry related directions.

states at non-zero frequencies exhibit different characteristic spatial patterns. The impurity resonance shown in Fig. 2(b) extends along the (100) -direction outside the square with a “V-like” fine structure consisting of branches that run along the (110) -direction. In contrast, the impurity state shown in Fig. 2(c) and (d) is “star-like” and extends almost radially outwards. Note that the “global” (i.e., larger length scale) spatial structure of the DOS at $\omega = \pm 5$ meV [Figs. 2(c) and (d)] is identical, and thus particle-hole symmetric. This symmetry also exists for other impurity resonances, such as the ones at $\omega = \pm 11$ meV. Only in the local, i.e., small length scale structure of the impurity resonance can we identify differences in the spatial DOS pattern. Of particular interest is the (local) 45° rotation of the DOS intensity between particle-like and hole-like energies in the vicinity of the nanostructure, which is similar to that observed near single impurities in the cuprate superconductors [2]. We find that the dichotomy of global particle-hole symmetry and local particle-hole asymmetry of impurity resonances is also exhibited by other nanostructure geometries.

When the square is rotated by 45° such that its sides are parallel to the (100) direction [see Fig. 3], specularly reflected electrons do not experience a sign change in the superconducting pairing potential and hence no impurity resonances are formed. This orientational dependence of the impurity resonances demonstrates that nanostructures are a new tool to identify the symmetry of unconventional superconductors in general. We find, however, that if an eigenmode of the nanostructure exists in the normal state at energies $|\omega| < \Delta_0$, the same eigenmode can also be excited in the superconducting state. Con-

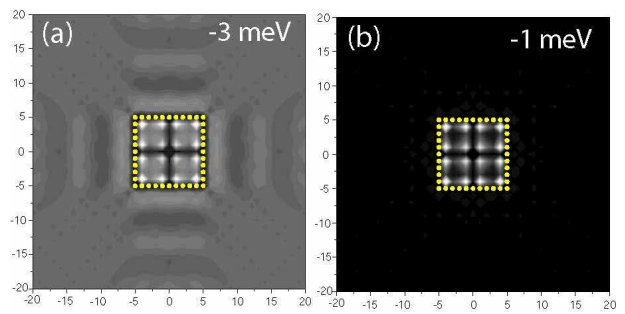


FIG. 3: Intensity plot of the DOS for a square with $N = 40$ impurities in (a) the normal state, and (b) the superconducting state.

sider for example the normal state eigenmode at $\omega = -3$ meV shown in Fig. 3(a). In the superconducting state, the same eigenmode is excited at $\omega = -1$ meV, as shown in Fig. 3(b). Note that this eigenmode in the superconducting state does *not* arise from pairbreaking effects, such as for example, the impurity *pairbreaking* resonances shown in Figs. 1(a),(b). It is therefore important to distinguish between impurity states that arise from eigenmodes of the nanostructure and those that are pairbreaking resonances. The spatial structure of impurity states is often determined by an interplay of eigenmodes and pairbreaking resonances, with eigenmodes (pairbreaking resonances) determining the spatial DOS pattern inside (outside of) the nanostructure.

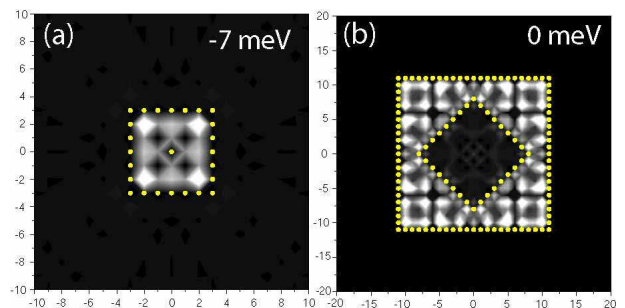


FIG. 4: Intensity plot of the DOS for (a) a screened single impurity, and (b) a screened impurity square (see text).

The fact that impurity states are absent for nanostructure squares whose sides are parallel to the (100) -direction can be used to “screen” impurity states in the superconducting state. For example, when a single impurity is enclosed by a square, as shown Fig. 4(a), the impurity state is completely confined to the interior of the square. This screening process considerably reduces the spatial extent of the impurity resonance, as follows from a comparison of Figs. 1(a) and 4(a). Even the more complex ZBCP-like state of Fig. 2(a) can be screened when enclosed by a second square, as shown in Fig. 4(b).

Ellipses, whose major axis are aligned along the (110) -direction, also possess ZBCP-like impurity states, as

shown in Fig. 5(a) and (b). In particular, at $\omega = 0$ meV, the impurity state permeates the entire ellipse along the minor axis of the ellipse. In contrast, at $\omega = -2$ meV, the impurity resonance outside the ellipse extends parallel to its minor axis, while in the ellipse's interior, it extends along its major axis. These ZBCP-like resonances are absent when the axes of the ellipse are parallel to the (100)-direction. More complex nanostructures provide the pos-

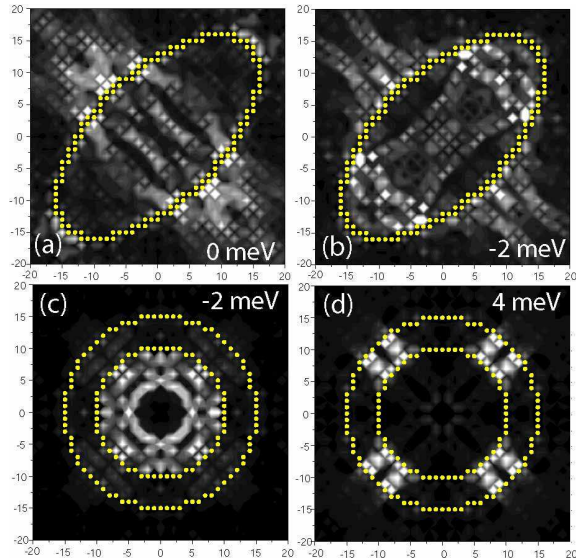


FIG. 5: Intensity plot of the DOS for (a),(b) an elliptical quantum corral with $N = 84$ impurities, whose axes of length $a = 20$ and $b = 10$ are aligned along the (110)-direction, and (c),(d) two congruent circles with radii $R_1 = 10$ and $R_2 = 15$ and $N = 141$ impurities.

sibility to create impurity resonances that are confined to distinctively different parts of the nanostructure. For example, the nanostructure consisting of two congruent circles shown in Figs. 5(c) and (d), possesses an impurity resonance at $\omega = -2$ meV [Figs. 5(c)] that is located predominantly inside the inner circle, while the one at $\omega = 4$ meV [Fig. 5(d)] which is reminiscent of the ZBCP, is confined to the area between the two circles. This result exemplifies the possibility to “custom-design” the spatial structure of impurity resonances, with the potential of gaining further insight into the complex electronic structure of the cuprates.

Since non-magnetic impurities are pair-breaking in a $d_{x^2-y^2}$ -wave superconductor, we expect that nanostructures also lead to a spatial variation of the superconducting order parameter. The effects of this spatial variation are beyond the scope of the present work, but will be addressed in future work within the self-consistent Bogoliubov de Gennes formalism. Our study of nanostructures in s -wave superconductors, however, has shown that such a spatial variation leads only to small quantitative changes from the results of the \hat{T} -matrix theory [15]. We therefore expect that our above results remain

qualitatively unchanged when the spatial variation of the superconducting order parameter is taken into account.

In summary, we have studied the effects of nanostructures on the local electronic structure of a $d_{x^2-y^2}$ -wave superconductor. We show that the interplay between the geometry of the nanostructure, its orientation and the momentum dependence of the superconducting gap gives rise to a series of interesting quantum effects, such as the emergence of ZBCP-like states and the screening of impurity resonances. These effects demonstrate that nanostructures are a new tool for identifying the symmetry of unconventional superconductors and for probing the electronic correlations of complex systems.

We would like to thank J.C. Davis for stimulating discussions. D.K.M. acknowledges financial support from the Alexander von Humboldt foundation.

-
- [1] A. Yazdani *et al.*, Phys. Rev. Lett. **83**, 176 (1999); S.H. Pan *et al.*, Nature (London) **403**, 746 (2000); D.J. Derro *et al.*, Phys. Rev. Lett. **88**, 097002 (2002).
 - [2] E.W. Hudson *et al.*, Nature (London) **411**, 920 (2001).
 - [3] M.I. Salkola, *et al.*, Phys. Rev. Lett. **77**, 1841 (1996).
 - [4] M.E. Flatte, and J.M. Byers, Phys. Rev. Lett. **78**, 3761 (1997); S. Haas and K. Maki, Phys. Rev. Lett. **85**, 2172 (2000); H. Tsuchiura *et al.*, Phys. Rev. Lett. **84**, 3165 (2000); J.-X. Zhu and C.S. Ting, Phys. Rev. B **64**, 060501(R) (2001).
 - [5] A. V. Balatsky, I. Vekhter, Jian-Xin Zhu, preprint, cond-mat/0411318.
 - [6] D.K. Morr and N. Stavropoulos, Phys. Rev. B **66**, 140508(R) (2002); L.Y. Zhu *et al.*, Phys. Rev. B **67**, 094508 (2003); B.M. Andersen and P. Hedegard, Phys. Rev. B **67**, 172505 (2003).
 - [7] H.C. Manoharan, C.P. Lutz, and D.M. Eigler, Nature (London) **403**, 512 (2000).
 - [8] G.A. Fiete *et al.*, Phys. Rev. Lett. **86**, 2392 (2001); A.A. Aligia, Phys. Rev. B **64**, 121102 (2001); K. Hallberg, A.A. Correa, and C.A. Balseiro, Phys. Rev. Lett. **88**, 066802 (2002); D. Porras *et al.*, Phys. Rev. B **63**, 155406 (2001); O. Agam and A. Schiller, Phys. Rev. Lett. **86**, 484 (2001); Y. Shimada *et al.*, Surf. Sci **514**, 89 (2002); M. Weissmann and H. Bonadeo, Physica E **10**, 544 (2001); M. Schmid and A.P. Kampf, Ann. Phys. **12**, 463 (2003).
 - [9] For a general review see G.A. Fiete and E.J. Heller, Rev. Mod. Phys. **75** 933 (2003), and references therein.
 - [10] D. K. Morr and N. A. Stavropoulos, Phys. Rev. Lett. **92**, 107006 (2004); *ibid.* Phys. Rev. B **71**, 140501(R) (2005).
 - [11] D. K. Morr and N. A. Stavropoulos, Phys. Rev. Lett. **92**, 107006 (2004); *ibid.*, Phys. Rev. B **67**, 020502(R) (2003).
 - [12] Y. Lu, Acta Physics Sinica **21**, 75 (1965); H. Shiba, Prog. Theoret. Phys. **40**, 435 (1968).
 - [13] A. Damascelli, Z. Hussain, and Z.-X. Shen, Rev. Mod. Phys. **75**, 473 (2003).
 - [14] J. Lesueur *et al.*, Physica C **191**, 325 (1992); J. Geerk *et al.*, Z. Phys. **73**, 329 (1994); M. Covington *et al.*, Appl. Phys. Lett. **68**, 1717 (1996); L. Alf *et al.*, Phys. Rev. B **55**, R14757 (1997).
 - [15] J. Yoon and D.K. Morr, in preparation.